

RESTRUCTURING VECTOR QUANTIZATION WITH THE ROTATION TRICK

Christopher Fifty¹, Ronald G. Junkins¹, Dennis Duan^{1,2}, Aniketh Iger¹, Jerry W. Liu¹, Ehsan Amid², Sebastian Thrun¹, Christopher Ré¹

¹Stanford University, ²Google DeepMind

fifty@cs.stanford.com

ABSTRACT

Vector Quantized Variational AutoEncoders (VQ-VAEs) are designed to compress a continuous input to a discrete latent space and reconstruct it with minimal distortion. They operate by maintaining a set of vectors—often referred to as the codebook—and quantizing each encoder output to the nearest vector in the codebook. However, as vector quantization is non-differentiable, the gradient to the encoder flows *around* the vector quantization layer rather than *through* it in a straight-through approximation. This approximation may be undesirable as all information from the vector quantization operation is lost. In this work, we propose a way to propagate gradients through the vector quantization layer of VQ-VAEs. We smoothly transform each encoder output into its corresponding codebook vector via a rotation and rescaling linear transformation that is treated as a constant during backpropagation. As a result, the relative magnitude and angle between encoder output and codebook vector becomes encoded into the gradient as it propagates through the vector quantization layer and back to the encoder. Across 11 different VQ-VAE training paradigms, we find this restructuring improves reconstruction metrics, codebook utilization, and quantization error. Our code is available at https://github.com/cfifty/rotation_trick.

1 INTRODUCTION

Vector quantization (Gray, 1984) is an approach to discretize a continuous vector space. It defines a finite set of vectors—referred to as the codebook—and maps any vector in the continuous vector space to the closest vector in the codebook. However, deep learning paradigms that use vector quantization are often difficult to train because replacing a vector with its closest codebook counterpart is a non-differentiable operation (Huh et al., 2023). This characteristic was not an issue at its creation during the Renaissance of Information Theory for applications like noisy channel communication (Cover, 1999); however in the era of deep learning, it presents a challenge as gradients cannot directly flow through layers that use vector quantization during backpropagation.

In deep learning, vector quantization is largely used in the eponymous Vector Quantized-Variational AutoEncoder (VQ-VAE) (Van Den Oord et al., 2017). A VQ-VAE is an AutoEncoder with a vector quantization layer between the encoder’s output and decoder’s input, thereby quantizing the learned representation at the bottleneck. While VQ-VAEs are ubiquitous in state-of-the-art generative modeling (Rombach et al., 2022; Dhariwal et al., 2020; Brooks et al., 2024), their gradients cannot flow from the decoder to the encoder uninterrupted as they must pass through a non-differentiable vector quantization layer.

A solution to the non-differentiability problem is to approximate gradients via a “straight-through estimator” (STE) (Bengio et al., 2013). During backpropagation, the STE copies and pastes the gradients from the decoder’s input to the encoder’s output, thereby skipping the quantization operation altogether. However, this approximation can lead to poor-performing models and codebook collapse: a phenomena where a large percentage of the codebook converge to zero norm and are unused by the model (Mentzer et al., 2023). Even if codebook collapse does not occur, the codebook is often under-utilized, thereby limiting the information capacity of the VQ-VAEs’s bottleneck (Dhariwal et al., 2020).

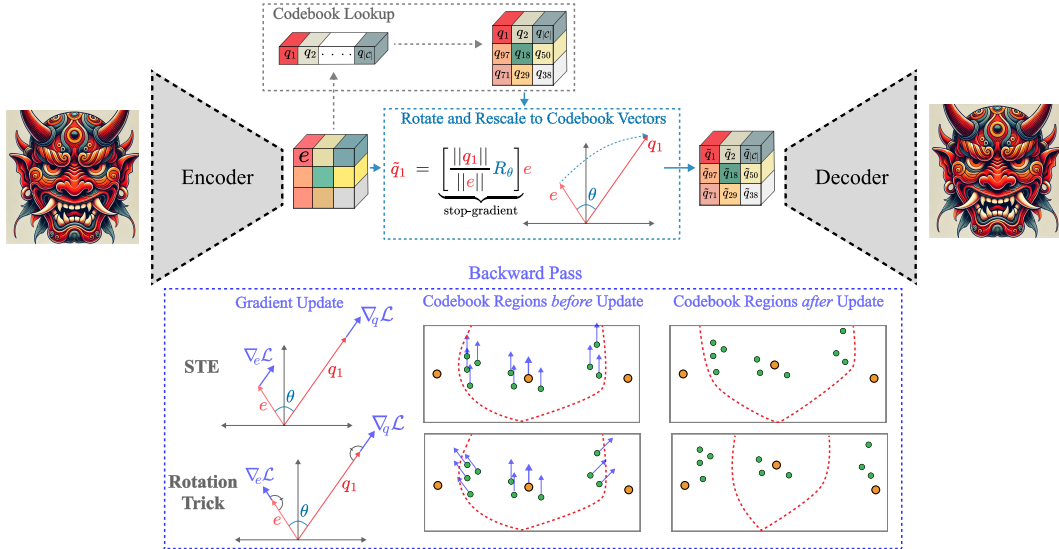


Figure 1: Illustration of the rotation trick. In the forward pass, encoder output e is rotated and rescaled to q_1 . Not shown is the rotation of the other encoder outputs to their corresponding codebook vectors. In the backward pass, the gradient at q_1 moves to e so that the angle between $\nabla_{q_1} \mathcal{L}$ and q_1 is preserved. Now, points within the same codebook region receive different gradients depending on their relative angle and magnitude to the codebook vector. For example, points with high angular distance can be *pushed* into new codebook regions, thereby increasing codebook utilization.

In this work, we propose an alternate way to propagate gradients through the vector quantization layer in VQ-VAEs. For a given encoder output e and nearest codebook vector q , we smoothly transform e to q via a rotation and rescaling linear transformation and then send this output—rather than the direct result of the codebook lookup—to the decoder. As the input to the decoder, \tilde{q} , is now treated as a smooth linear transformation of e , gradients flow back from the decoder to the encoder unimpeded. To avoid differentiating through the rotation and rescaling, we treat both as constants with respect to e and q . We explain why this choice is necessary in Appendix A.2. Following the convention of Kingma & Welling (2013), we call this restructuring “the rotation trick.” It is illustrated in Figure 3 and described in Algorithm 1.

The rotation trick does not change the output of the VQ-VAE in the forward pass. However, during the backward pass, it transports the gradient $\nabla_q \mathcal{L}$ at q to become the gradient $\nabla_e \mathcal{L}$ at e so that the angle between q and $\nabla_q \mathcal{L}$ after the vector quantization layer equals the angle between e and $\nabla_e \mathcal{L}$ before the vector quantization layer. Preserving this angle encodes relative angular distances and magnitudes into the gradient and changes how points within the same codebook region are updated.

The STE applies the same update to all points within the same codebook region, maintaining their relative distances. However as we will show in Section 4.3, the rotation trick can push points within the same codebook region farther apart—or pull them closer together—depending on the direction of the gradient vector. The former capability can correspond to increased codebook usage while the latter to lower quantization error. In the context of lossy compression, both capabilities are desirable for reducing the distortion and increasing the information capacity of the vector quantization layer.

When applied to several open-source VQ-VAE repositories, we find the rotation trick substantively improves reconstruction performance, increases codebook usage, and decreases the distance between encoder outputs and their corresponding codebook vectors. For instance, training the VQGAN from Rombach et al. (2022) on ImageNet (Deng et al., 2009) with the rotation trick improves reconstruction FID from 5.0 to 1.6, reconstruction IS from 141.5 to 190.3, increases codebook usage from 2% to 9%, and decreases quantization error by over an order of magnitude.

2 RELATED WORK

Many researchers have built upon the seminal work of [Van Den Oord et al. \(2017\)](#) to improve VQ-VAE performance. While non-exhaustive, our review focuses on methods that address training instabilities caused by the vector quantization layer. We partition these efforts into two categories: (1) methods that sidestep the STE and (2) methods that improve codebook-model interactions.

Sidestepping the STE. Several prior works have sought to fix the problems caused by the STE by avoiding deterministic vector quantization. [Baevski et al. \(2019\)](#) employ the Gumbel-Softmax trick ([Jang et al., 2016](#)) to fit a categorical distribution over codebook vectors that converges to a one-hot distribution towards the end of training, [Gautam et al. \(2023\)](#) quantize using a convex combination of codebook vectors, and [Takida et al. \(2022\)](#) employ stochastic quantization. Unlike the above that cast vector quantization as a distribution over codebook vectors, [Huh et al. \(2023\)](#) propose an alternating optimization where the encoder is optimized to output representations close to the codebook vectors while the decoder minimizes reconstruction loss from a fixed set of codebook vector inputs. While these approaches sidestep the training instabilities caused by the STE, they can introduce their own set of problems and complexities such as low codebook utilization at inference and the tuning of a temperature schedule ([Zhang et al., 2023](#)). As a result, many applications and research papers continue to employ VQ-VAEs that are trained using the STE ([Rombach et al., 2022](#); [Chang et al., 2022](#); [Huang et al., 2023](#); [Zhu et al., 2023](#); [Dong et al., 2023](#)).

Codebook-Model Improvements. Another way to attack codebook collapse or under-utilization is to change the codebook lookup. Rather than use Euclidean distance, [Yu et al. \(2021\)](#) employ a cosine similarity measure, [Goswami et al. \(2024\)](#) a hyperbolic metric, and [Lee et al. \(2022\)](#) stochastically sample codes as a function of the distance between the encoder output and codebook vectors. Another perspective examines the learning of the codebook. [Kolesnikov et al. \(2022\)](#) split high-usage codebook vectors, [Dhariwal et al. \(2020\)](#); [Łańcucki et al. \(2020\)](#); [Zheng & Vedaldi \(2023\)](#) resurrect low-usage codebook vectors throughout training, [Chen et al. \(2024\)](#) dynamically selects one of m codebooks for each datapoint, and [Mentzer et al. \(2023\)](#); [Zhao et al. \(2024\)](#); [Yu et al. \(2023\)](#); [Chiu et al. \(2022\)](#) fix the codebook vectors to an *a priori* geometry and train the model without learning the codebook at all. Other works propose loss penalties to encourage codebook utilization. [Zhang et al. \(2023\)](#) add a KL-divergence penalty between codebook utilization and a uniform distribution while [Yu et al. \(2023\)](#) add an entropy loss term to penalize low codebook utilization. While effective at targeting specific training difficulties, as each of these methods continue to use the STE, the training instability caused by this estimator persist. Most of our experiments in Section 5 implement a subset of these approaches, and we find that replacing the STE with the rotation trick further improves performance.

3 STRAIGHT THROUGH ESTIMATOR (STE)

In this section, we review the Straight-Through Estimator (STE) and visualize its effect on the gradients. We then explore two STE alternatives that—at first glance—appear to correct the approximation made by the STE.

For notation, we define a sample space \mathcal{X} over the input data with probability distribution p . For input $x \in \mathcal{X}$, we define the encoder as a deterministic mapping that parameterizes a posterior distribution $p_{\mathcal{E}}(e|x)$. The vector quantization layer, $\mathcal{Q}(\cdot)$, is a function that selects the codebook vector $q \in \mathcal{C}$ nearest to the encoder output e . Under Euclidean distance, it has the form:

$$\mathcal{Q}(q = i|e) = \begin{cases} 1 & \text{if } i = \arg \min_{1 \leq j \leq |\mathcal{C}|} \|e - q_j\|_2 \\ 0 & \text{otherwise} \end{cases}$$

The decoder is similarly defined as a deterministic mapping that parameterizes the conditional distribution over reconstructions $p_{\mathcal{D}}(\tilde{x}|q)$. As in the VAE ([Kingma & Welling, 2013](#)), the loss function follows from the ELBO with the KL-divergence term zeroing out as $p_{\mathcal{E}}(e|x)$ is deterministic and the utilization over codebook vectors is assumed to be uniform. [Van Den Oord et al. \(2017\)](#) additionally add a “codebook loss” term $\|sg(e) - q\|_2^2$ to learn the codebook vectors and a “commitment loss” term $\beta\|e - sg(q)\|_2^2$ to pull the encoder’s output towards the codebook vectors. sg stands for stop-gradient and β is a hyperparameter, typically set to a value in $[0.25, 2]$. For predicted reconstruction \tilde{x} , the optimization objective becomes:

$$\mathcal{L}(\tilde{x}) = \|x - \tilde{x}\|_2^2 + \|sg(e) - q\|_2^2 + \beta\|e - sg(q)\|_2^2$$

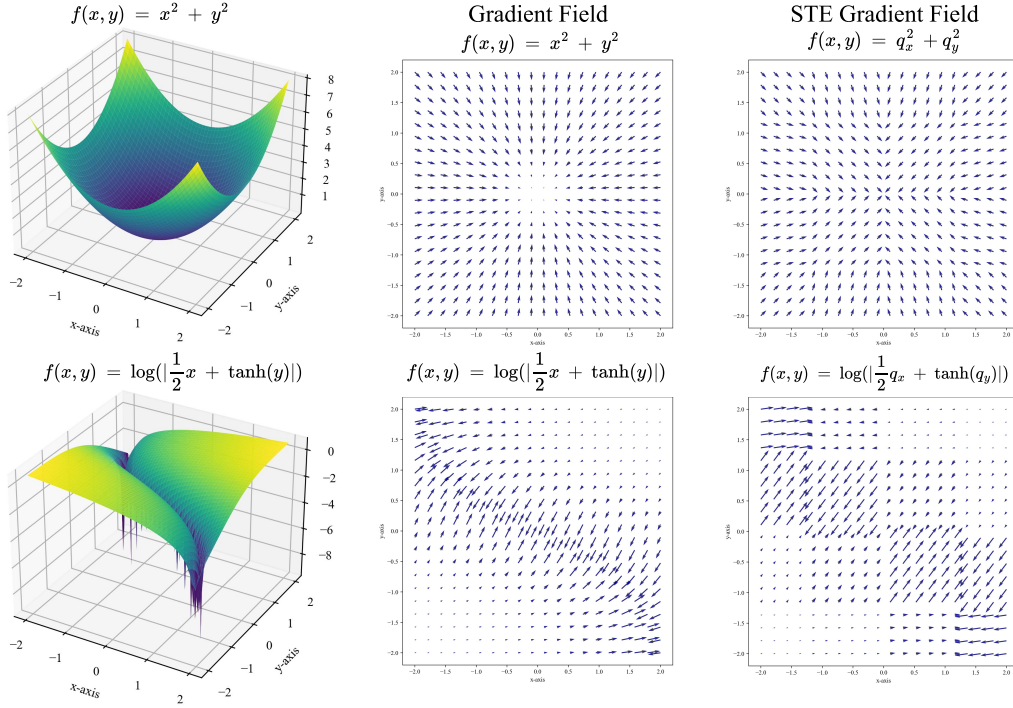


Figure 2: Visualization of how the straight-through estimator (STE) transforms the gradient field for 16 codebook vectors for (top) $f(x, y) = x^2 + y^2$ and (bottom) $f(x, y) = \log\left(\left|\frac{1}{2}x + \tanh(y)\right|\right)$. The STE takes the gradient at the codebook vector (q_x, q_y) and “copies-and-pastes” it to all other locations within the same codebook region, forming a “checker-board” pattern in the gradient field.

In the subsequent analysis, we focus only on the $\|x - \tilde{x}\|_2^2$ term as the other two are not functions of the decoder. During backpropagation, the model must differentiate through the vector quantization function $\mathcal{Q}(\cdot)$. We can break down the backward pass into three terms:

$$\frac{\partial \mathcal{L}}{\partial x} = \frac{\partial \mathcal{L}}{\partial q} \frac{\partial q}{\partial e} \frac{\partial e}{\partial x}$$

where $\frac{\partial \mathcal{L}}{\partial q}$ represents backpropagation through the decoder, $\frac{\partial q}{\partial e}$ represents backpropagation through the vector quantization layer, and $\frac{\partial e}{\partial x}$ represents backpropagation through the encoder. As vector quantization is not a smooth transformation, $\frac{\partial q}{\partial e}$ cannot be computed and gradients cannot flow through this term to update the encoder in backpropagation.

To solve the issue of non-differentiability, the STE copies the gradients from q to e , bypassing vector quantization entirely. Simply, the STE sets $\frac{\partial q}{\partial e}$ to the identity matrix I in the backward pass:

$$\frac{\partial \mathcal{L}}{\partial x} = \frac{\partial \mathcal{L}}{\partial q} I \frac{\partial e}{\partial x}$$

The first two terms $\frac{\partial \mathcal{L}}{\partial q} \frac{\partial q}{\partial e}$ combine to $\frac{\partial \mathcal{L}}{\partial e}$ which, somewhat misleadingly, does not actually depend on e . As a consequence, the location of e within the Voronoi partition generated by codebook vector q —be it close to q or at the boundary of the region—has no impact on the gradient update to the encoder.

An example of this effect is visualized in Figure 2 for two example functions. In the STE approximation, the “exact” gradient at the encoder output is replaced by the gradient at the corresponding codebook vector for each Voronoi partition, irrespective of where in that region the encoder output e lies. As a result, the exact gradient field becomes “partitioned” into 16 different regions—all with the same gradient update to the encoder—for the 16 vectors in the codebook.

Returning to our question, is there a better way to propagate gradients through the vector quantization layer? At first glance, one may be tempted to estimate the curvature at q and use this information to transform $\frac{\partial q}{\partial e}$ as q moves to e . This is accomplished by taking a second order expansion around q to

approximate the value of the loss at e :

$$\mathcal{L}_e \approx \mathcal{L}_q + (\nabla_q \mathcal{L})^T(e - q) + \frac{1}{2}(e - q)^T(\nabla_q^2 \mathcal{L})(e - q)$$

Then we can compute the gradient at the point e instead of q up to second order approximation with:

$$\begin{aligned} \frac{\partial \mathcal{L}}{\partial e} &\approx \frac{\partial}{\partial e} \left[\mathcal{L}_q + (\nabla_q \mathcal{L})^T(e - q) + \frac{1}{2}(e - q)^T(\nabla_q^2 \mathcal{L})(e - q) \right] \\ &= \nabla_q \mathcal{L} + (\nabla_q^2 \mathcal{L})(e - q) \end{aligned}$$

While computing Hessians with respect to model parameters are typically prohibitive in modern deep learning architectures, computing them with respect to only the codebook is feasible. Moreover as we must only compute $(\nabla_q^2 \mathcal{L})(e - q)$, one may take advantage of efficient Hessian-Vector products implementations in deep learning frameworks (Dagréou et al., 2024) and avoid computing the full Hessian matrix.

Extending this idea a step further, we can compute the exact gradient $\frac{\partial \mathcal{L}}{\partial e}$ at e by making two passes through the network. Let \mathcal{L}_q be the loss with the vector quantization layer and \mathcal{L}_e be the loss without vector quantization, i.e. $q = e$ rather than $q = \mathcal{Q}(e)$. Then one may form the total loss $\mathcal{L} = \mathcal{L}_q + \lambda \mathcal{L}_e$, where λ is a small constant like 10^{-6} , to scale down the effect of \mathcal{L}_e on the decoder’s parameters and use a gradient scaling multiplier of λ^{-1} to reweigh the effect of \mathcal{L}_e on the encoder’s parameters to 1. As $\frac{\partial q}{\partial e}$ is non-differentiable, gradients from \mathcal{L}_q will not flow to the encoder.

While seeming to correct the encoder’s gradients, replacing the STE with either approach will likely result in worse performance. This is because computing the exact gradient with respect to e is actually the AutoEncoder (Hinton & Zemel, 1993) gradient, the model that VAEs (Kingma & Welling, 2013) and VQ-VAEs (Van Den Oord et al., 2017) were designed to replace given the AutoEncoder’s propensity to overfit and difficultly generalizing. Accordingly using either Hessian approximation or exact gradients via a double forward pass will cause the encoder to be trained like an AutoEncoder and the decoder to be trained like a VQ-VAE. This mis-match in optimization objectives is likely another contributing factor to the poor performance we observe for both methods in Table 1.

4 THE ROTATION TRICK

As discussed in Section 3, updating the encoder’s parameters by approximating, or exactly, computing the gradient at the encoder’s output is undesirable. Similarly, the STE appears to lose information: the location of e within the quantized region—be it close to q or far away at the boundary—has no impact on the gradient update to the encoder. Capturing this information, i.e. using the location of e in relation to q to transform the gradients through $\frac{\partial q}{\partial e}$, could be beneficial to the encoder’s gradient updates and an improvement over the STE.

Viewed geometrically, we ask how to move the gradient $\nabla_q \mathcal{L}$ from q to e , and what characteristics of $\nabla_q \mathcal{L}$ and q should be preserved during this movement. The STE offers one possible answer: move the gradient from q to e so that its direction and magnitude are preserved. However, this paper supplies a different answer: move the gradient so that the angle between $\nabla_q \mathcal{L}$ and q is preserved as $\nabla_q \mathcal{L}$ moves to e . We term this approach “the rotation trick”, and in Section 4.3 we show that preserving the angle between q and $\nabla_q \mathcal{L}$ conveys desirable properties to how points move within the same quantized region.

4.1 THE ROTATION TRICK PRESERVES ANGLES

In this section, we formally define the rotation trick. For encoder output e , let $q = \mathcal{Q}(e)$ represent the corresponding codebook vector. $\mathcal{Q}(\cdot)$ is non-differentiable so gradients cannot flow through this layer during the backward pass. The STE solves this problem—maintaining the direction and magnitude of the gradient $\nabla_q \mathcal{L}$ —as $\nabla_q \mathcal{L}$ moves from q to e with some clever hacking of the backpropagation function in deep learning frameworks:

$$\tilde{q} = e - \underbrace{(q - e)}_{\text{constant}}$$

which is a parameterization of vector quantization that sets the gradient at the encoder output to the gradient at the decoder’s input. The rotation trick offers a different parameterization: casting the forward pass as a rotation and rescaling that aligns e with q :

$$\tilde{q} = \left[\frac{\|q\|}{\|e\|} R \right] e$$

constant

R is the rotation¹ transformation that aligns e with q and $\frac{\|q\|}{\|e\|}$ rescales e to have the same magnitude as q . Note that both R and $\frac{\|q\|}{\|e\|}$ are functions of e . To avoid differentiating through this dependency, we treat them as fixed constants—or detached from the computational graph in deep learning frameworks—when differentiating. This choice is explained in Appendix A.2.

While the rotation trick does not change the output of the forward pass, the backward pass changes. Rather than set $\frac{\partial q}{\partial e} = I$ as in the STE, the rotation trick sets $\frac{\partial q}{\partial e}$ to be a rotation and rescaling transformation:

$$\frac{\partial \tilde{q}}{\partial e} = \frac{\|q\|}{\|e\|} R$$

As a result, $\frac{\partial q}{\partial e}$ changes based on the position of e in the codebook partition of q , and notably, the angle between $\nabla_q \mathcal{L}$ and q is preserved as $\nabla_q \mathcal{L}$ moves to e . This effect is visualized in Figure 3. While the STE translates the gradient from q to e , the rotation trick rotates it so that the angle between $\nabla_q \mathcal{L}$ and q is preserved. In a sense, the rotation trick and the STE are siblings. They choose different characteristics of the gradient as desiderata and then preserve those characteristics as the gradient flows around the non-differentiable vector quantization operation to the encoder.

4.2 EFFICIENT ROTATION COMPUTATION

The rotation transformation R that rotates e to q can be efficiently computed with Householder matrix reflections. We define $\hat{e} = \frac{e}{\|e\|}$, $\hat{q} = \frac{q}{\|q\|}$, $\lambda = \frac{\|q\|}{\|e\|}$, and $r = \frac{\hat{e} + \hat{q}}{\|\hat{e} + \hat{q}\|}$. Then the rotation and rescaling that aligns e to q is simply:

$$\begin{aligned} \tilde{q} &= \lambda R e \\ &= \lambda(I - 2rr^T + 2\hat{q}\hat{e}^T)e \\ &= \lambda[e - 2rr^T e + 2\hat{q}\hat{e}^T e] \end{aligned}$$

Due to space constraints, we leave the derivation of this formula to Appendix A.4. Parameterizing the rotation in this fashion avoids computing outer products and therefore consumes minimal GPU VRAM. Further, we did not detect a difference in wall-clock time between VQ-VAEs trained with the STE and VQ-VAEs trained with the rotation trick for our experiments in Section 5.

4.3 VORONOI PARTITION ANALYSIS

In the context of lossy compression, vector quantization works well when the distortion, or equivalently quantization error $\|e - q\|_2^2$, is low and the information capacity—equivalently codebook utilization—is high (Cover, 1999). Later in Section 5, we will see that VQ-VAEs trained with the rotation trick have this *desiderata*—often reducing quantization error by an order of magnitude and substantially increasing codebook usage—when compared to VQ-VAEs trained with the STE. However, the underlying reason *why* this occurs is less clear.

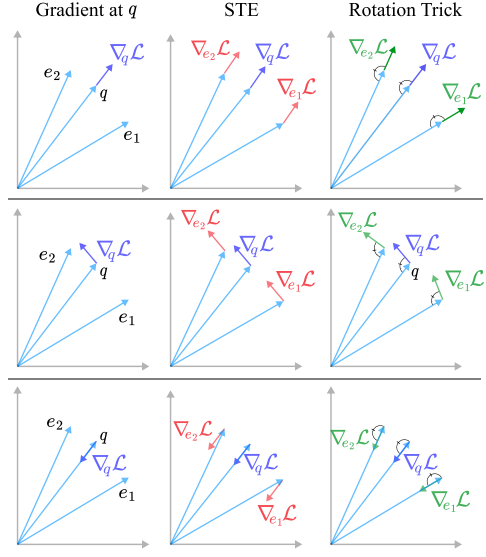


Figure 3: Illustration of how the gradient at q moves to e via the STE (middle) and rotation trick (right). The STE “copies-and-pastes” the gradient to preserve its direction while the rotation trick moves the gradient so the angle between q and $\nabla_q \mathcal{L}$ is preserved.

¹A rotation is defined as a linear transformation so that $RR^T = I$, $R^{-1} = R^T$, and $\det(R) = 1$.

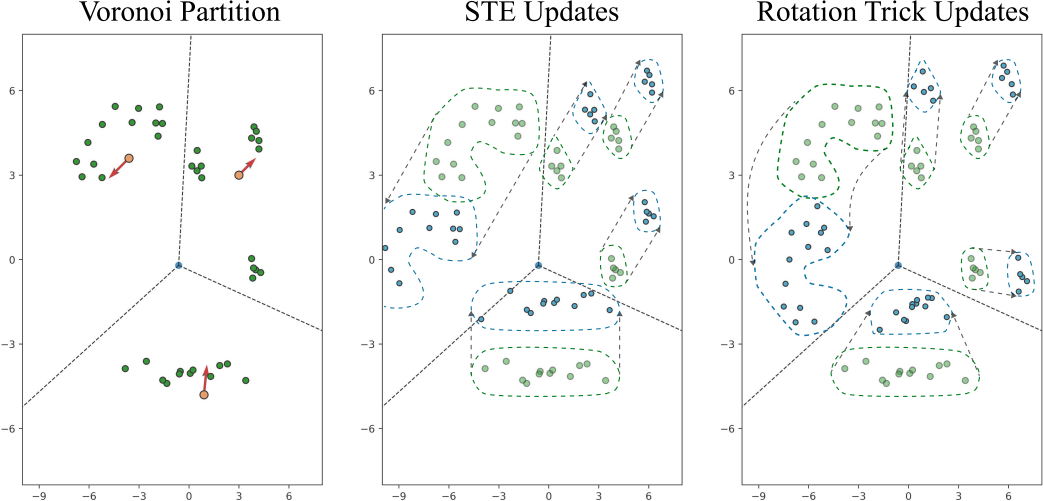


Figure 4: Depiction of how points within the same codebook region change after a gradient update (red arrow) at the codebook vector (orange circle). The STE applies the same update to each point in the same region. The rotation trick modifies the update based on the location of each point with respect to the codebook vector.

In this section, we analyze the effect of the rotation trick by looking at how encoder outputs that are mapped to the same Voronoi region are updated. While the STE applies the same update to all points within the same partition, the rotation trick changes the update based on the location of points within the Voronoi region. It can push points within the same region farther apart or pull them closer together depending on the direction of the gradient vector. The former capability can correspond to increased codebook usage while the latter to lower quantization error.

Let θ be the angle between e and q and $\tilde{\theta}$ be the angle between q and $\nabla_q \mathcal{L}$. Intuitively, when θ is large, e maps to q with high distortion. In this case, we'd like e to commit one way or another. Either (1) make e commit to its current codebook vector by **pulling** e closer to q or (2) **push** e to a different codebook vector entirely. This behavior is preferable to maintaining states of high distortion where the distance between e and q remains constant. We will show the rotation trick enables both (1) and (2); however, the STE perpetuates the latter as visualized in Figure 5.

When $\nabla_q \mathcal{L}$ and q point in the same direction, i.e. $-\pi/2 < \tilde{\theta} < \pi/2$, encoder outputs with large angular distance to q are pushed *further* away than they would otherwise be moved by the STE update. Figure 5 illustrates this effect. The points with large angular distance (blue regions) move further away from q than the points with low angular distance (ivory regions).

The top right partitions of Figure 4 present an example of this effect. The two clusters of points at the boundary—with relatively large angle to the codebook vector—are pushed away while the cluster of points with small angle to the codebook vector move with it. The ability to push points at the boundary out of a quantized region and into another is desirable for increasing codebook utilization. Specifically, codebook utilization improves when points are pushed into the Voronoi regions of previously unused codebook vectors. This capability is not shared by the STE, which moves all points in the same region by the same amount.

When $\nabla_q \mathcal{L}$ and q point in opposite directions, i.e. $\pi/2 < \tilde{\theta} < 3\pi/2$, the distance among points within the same Voronoi region decreases as they are pulled towards the location of the updated codebook vector. This effect is visualized in Figure 5 (green regions) and the bottom partitions of Figure 4 show an example. Unlike the STE update—that maintains the distances among points—the rotation trick pulls points with high

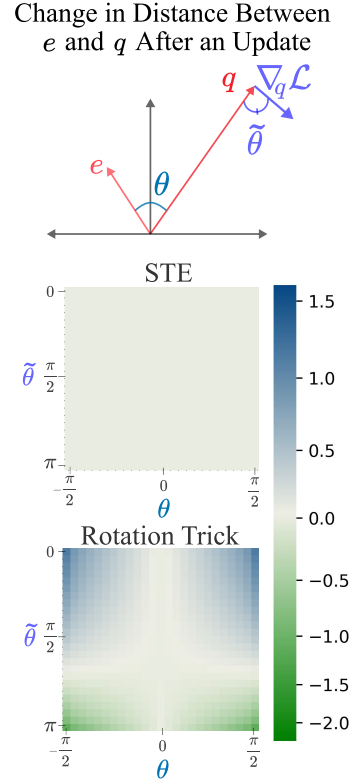


Figure 5: With the STE, the distances among points within the same region do not change. However with the rotation trick, the distances among points *do* change. When $\tilde{\theta} < \pi/2$, points with large angular distance are pushed away (blue: **increasing distance**). When $\tilde{\theta} > \pi/2$, points are *pulled* towards the codebook vector (green: **decreasing distance**).

Table 1: Comparison of VQ-VAEs trained on ImageNet following [Van Den Oord et al. \(2017\)](#). We use the Vector Quantization layer from <https://github.com/lucidrains/vector-quantize-pytorch>.

Approach	Training Metrics			Validation Metrics		
	Codebook Usage (\uparrow)	Rec. Loss (\downarrow)	Quantization Error (\downarrow)	Rec. Loss (\downarrow)	r-FID (\downarrow)	r-IS (\uparrow)
Codebook Lookup: Euclidean & Latent Shape: $32 \times 32 \times 32$ & Codebook Size: 1024						
VQ-VAE	100%	0.107	5.9e-3	0.115	106.1	11.7
VQ-VAE w/ Rotation Trick	97%	0.116	5.1e-4	0.122	85.7	17.0
Codebook Lookup: Cosine & Latent Shape: $32 \times 32 \times 32$ & Codebook Size: 1024						
VQ-VAE	75%	0.107	2.9e-3	0.114	84.3	17.7
VQ-VAE w/ Rotation Trick	91%	0.105	2.7e-3	0.111	82.9	18.1
Codebook Lookup: Euclidean & Latent Shape: $64 \times 64 \times 3$ & Codebook Size: 8192						
VQ-VAE	100%	0.028	1.0e-3	0.030	19.0	97.3
VQ-VAE w/ Hessian Approx.	39%	0.082	6.9e-5	0.112	35.6	65.1
VQ-VAE w/ Exact Gradients	84%	0.050	2.0e-3	0.053	25.4	80.4
VQ-VAE w/ Rotation Trick	99%	0.028	1.4e-4	0.030	16.5	106.3
Codebook Lookup: Cosine & Latent Shape: $64 \times 64 \times 3$ & Codebook Size: 8192						
VQ-VAE	31%	0.034	1.2e-4	0.038	26.0	77.8
VQ-VAE w/ Hessian Approx.	37%	0.035	3.8e-5	0.037	29.0	71.5
VQ-VAE w/ Exact Gradients	38%	0.035	3.6e-5	0.037	28.2	75.0
VQ-VAE w/ Rotation Trick	38%	0.033	9.6e-5	0.035	24.2	83.9

angular distances closer towards the post-update codebook vector. This capability is desirable for reducing the quantization error and enabling the encoder to *lock on* ([Van Den Oord et al., 2017](#)) to a target codebook vector.

Taken together, both capabilities can form a push-pull effect that achieves two *desiderata* of vector quantization: increasing information capacity and reducing distortion. Encoder outputs that have large angular distance to the chosen codebook vector are “pushed” to other, possibly unused, codebook regions by outwards-pointing gradients, thereby increasing codebook utilization. Concurrent with this effect, center-pointing gradients will “pull” points loosely clustered around the codebook vector closer together, locking on to the chosen codebook vector and reducing quantization error.

A third and final difference with the STE occurs when $\nabla_q \mathcal{L}$ is exactly orthogonal to q , i.e. $\tilde{\theta} = \pi/2$. For this event, each point within the Voronoi region generated by q is rotated by the same amount in the direction of $\nabla_q \mathcal{L}$. The top left Voronoi regions of Figure 4 visualize this case. While it is unlikely that the gradient is exactly orthogonal to the codebook vector, the gradient’s orthogonal component to q enables points to move in orthogonal directions via a rotation and expansion (if $\tilde{\theta} < \pi/2$) or a rotation and contraction (if $\tilde{\theta} > \pi/2$).

5 EXPERIMENTS

In Section 4.3, we showed the rotation trick enables behavior that would increase codebook utilization and reduce quantization error by changing how points within the same Voronoi region are updated. However, the extent to which these changes will affect applications is unclear. In this section, we evaluate the effect of the rotation trick across many different VQ-VAE paradigms.

We begin with image reconstruction: training a VQ-VAE with the reconstruction objective of [Van Den Oord et al. \(2017\)](#) and later extend our evaluation to the more complex VQGANs ([Esser et al., 2021](#)), the VQGANs designed for latent diffusion ([Rombach et al., 2022](#)), and then the ViT-VQGAN ([Yu et al., 2021](#)). Finally, we evaluate VQ-VAE reconstructions on videos using a TimeSformer ([Bertasius et al., 2021](#)) encoder and decoder. In total, our empirical analysis spans 11 different VQ-VAE configurations. For all experiments, aside from handling $\frac{\partial q}{\partial e}$ differently, the models, hyperparameters, and training settings are identical.

5.1 VQ-VAE EVALUATION

We begin with a straightforward evaluation: training a VQ-VAE to reconstruct examples from ImageNet ([Deng et al., 2009](#)). Following [Van Den Oord et al. \(2017\)](#), our training objective is a linear combination of the reconstruction, codebook, and commitment loss:

$$\mathcal{L} = \|x - \tilde{x}\|_2^2 + \|sg(e) - q\|_2^2 + \beta \|e - sg(q)\|_2^2$$

where β is a hyperparameter scaling constant. Following convention, we drop the codebook loss term from the objective and instead use an exponential moving average to update the codebook vectors.

Table 2: Results for VQGAN designed for autoregressive generation as implemented in <https://github.com/CompVis/taming-transformers>. Experiments on ImageNet and the combined dataset FFHQ (Karras et al., 2019) and CelebA-HQ (Karras, 2017) use a latent bottleneck of dimension $16 \times 16 \times 256$ with 1024 codebook vectors.

Approach	Dataset	Codebook Usage	Quantization Error (\downarrow)	Valid Loss (\downarrow)	r-FID (\downarrow)	r-IS (\uparrow)
VQGAN (reported)	ImageNet	—	—	—	7.9	114.4
VQGAN (our run)	ImageNet	95%	0.134	0.594	7.3	118.2
VQGAN w/ Rotation Trick	ImageNet	98%	0.002	0.422	4.6	146.5
VQGAN	FFHQ & CelebA-HQ	27%	0.233	0.565	4.7	5.0
VQGAN w/ Rotation Trick	FFHQ & CelebA-HQ	99%	0.002	0.313	3.7	5.2

Table 3: Results for VQGAN designed for latent diffusion as implemented in <https://github.com/CompVis/latent-diffusion>. Both settings train on ImageNet.

Approach	Latent Shape	Codebook Size	Codebook Usage	Quantization Error (\downarrow)	Valid Loss (\downarrow)	r-FID (\downarrow)	r-IS (\uparrow)
VQGAN	$64 \times 64 \times 3$	8192	15%	2.5e-3	0.183	0.53	220.6
VQGAN w/ Rotation Trick	$64 \times 64 \times 3$	8192	10%	2.9e-4	0.173	0.38	222.4
VQGAN	$32 \times 32 \times 4$	16384	2%	1.2e-2	0.385	5.0	141.5
VQGAN w/ Rotation Trick	$32 \times 32 \times 4$	16384	9%	7.2e-4	0.287	1.6	190.3

Evaluation Settings. For $256 \times 256 \times 3$ input images, we evaluate two different settings: (1) compressing to a latent space of dimension $32 \times 32 \times 32$ with a codebook size of 1024 following Yu et al. (2021) and (2) compressing to $64 \times 64 \times 3$ with a codebook size of 8192 following Rombach et al. (2022). In both settings, we compare with a Euclidean and cosine similarity codebook lookup.

Evaluation Metrics. We log both training and validation set reconstruction metrics. Of note, we compute reconstruction FID (Heusel et al., 2017) and reconstruction IS (Salimans et al., 2016) on reconstructions from the full ImageNet validation set as a measure of reconstruction quality. We also compute codebook usage, or the percentage of codebook vectors that are used in each batch of data, as a measure of the information capacity of the vector quantization layer and quantization error $\|e - q\|_2^2$ as a measure of distortion.

Baselines. Our comparison spans the STE estimator (VQ-VAE), the Hessian approximation described in Section 3 (VQ-VAE w/ Hessian Approx), the exact gradient backward pass described in Section 3 (VQ-VAE w/ Exact Gradients), and the rotation trick (VQ-VAE w/ Rotation Trick). All methods share the same architecture, hyperparameters, and training settings, and these settings are summarized in Table 6 of the Appendix. There is no functional difference among methods in the forward pass; the only differences relates to how gradients are propagated through $\frac{\partial q}{\partial e}$ during backpropagation.

Results. Table 1 displays our findings. We find that using the rotation trick reduces the quantization error—sometimes by an order of magnitude—and improves low codebook utilization. Both results are expected given the Voronoi partition analysis in Section 4.3: points at the boundary of quantized regions are likely pushed to under-utilized codebook vectors while points loosely grouped around the codebook vector are condensed towards it. These two features appear to have a meaningful effect on reconstruction metrics: training a VQ-VAE with the rotation trick substantially improves r-FID and r-IS.

We also see that the Hessian Approximation or using Exact Gradients results in poor reconstruction performance. While the gradients to the encoder are, in a sense, “more accurate”, training the encoder like an AutoEncoder (Hinton & Zemel, 1993) likely introduces overfitting and poor generalization. Moreover, the mismatch in training objectives between the encoder and decoder is likely an aggravating factor and partly responsible for both models’ poor performance.

5.2 VQGAN EVALUATION

Moving to the next level of complexity, we evaluate the effect of the rotation trick on VQGANs (Esser et al., 2021). The VQGAN training objective is:

$$\mathcal{L}_{\text{VQGAN}} = \mathcal{L}_{\text{Per}} + \|sg(e) - q\|_2^2 + \beta \|e - sg(q)\|_2^2 + \lambda \mathcal{L}_{\text{Adv}}$$

where \mathcal{L}_{Per} is the perceptual loss from Johnson et al. (2016) and replaces the L_2 loss used to train VQ-VAEs. \mathcal{L}_{Adv} is a patch-based adversarial loss similar to the adversarial loss in Conditional GAN (Isola et al., 2017). β is a constant that weights the commitment loss while λ is an adaptive weight based on the ratio of $\nabla \mathcal{L}_{\text{Per}}$ to $\nabla \mathcal{L}_{\text{Adv}}$ with respect to the last layer of the decoder.

Experimental Settings. We evaluate VQGANs under two settings: (1) the paradigm amenable to autoregressive modeling with Transformers as described in Esser et al. (2021) and (2) the paradigm suitable to latent diffusion models as described in Rombach et al. (2022). The first setting follows

Table 4: Results for ViT-VQGAN (Yu et al., 2021) trained on ImageNet. The latent shape is $8 \times 8 \times 32$ with 8192 codebook vectors. r-FID and r-IS are reported on the validation set.

Approach	Codebook Usage (\uparrow)	Train Loss (\downarrow)	Quantization Error (\downarrow)	Valid Loss (\downarrow)	r-FID (\downarrow)	r-IS (\uparrow)
ViT-VQGAN [reported]	—	—	—	—	22.8	72.9
ViT-VQGAN [ours]	0.3%	0.124	6.7e-3	0.127	29.2	43.0
ViT-VQGAN w/ Rotation Trick	2.2%	0.113	8.3e-3	0.113	11.2	93.1

Table 5: Results for TimeSformer-VQGAN trained on BAIR and UCF-101 with 1024 codebook vectors. \dagger : model suffers from codebook collapse and diverges. r-FVD is computed on the validation set.

Approach	Dataset	Codebook Usage	Train Loss (\downarrow)	Quantization Error (\downarrow)	Valid Loss (\downarrow)	r-FVD (\downarrow)
TimeSformer †	BAIR	0.4%	0.221	0.03	0.28	1661.1
TimeSformer w/ Rotation Trick	BAIR	43%	0.074	3.0e-3	0.074	21.4
TimeSformer †	UCF-101	0.1%	0.190	0.006	0.169	2878.1
TimeSformer w/ Rotation Trick	UCF-101	30%	0.111	0.020	0.109	229.1

the convolutional neural network and default hyperparameters described in Esser et al. (2021) while the second follows those from Rombach et al. (2022). A full description of both training settings is provided in Table 7 of the Appendix.

Results. Our results are listed in Table 2 for the first setting and Table 3 for the second. Similar to our findings in Section 5.1, we find that training a VQ-VAE with the rotation trick substantially decreases quantization error and often improves codebook usage. Moreover, reconstruction performance as measured on the validation set by the total loss, r-FID, and r-IS are significantly improved across both modeling paradigms.

5.3 ViT-VQGAN EVALUATION

Improving upon the VQGAN model, Yu et al. (2021) propose using a ViT (Dosovitskiy, 2020) rather than CNN to parameterize the encoder and decoder. The ViT-VQGAN uses factorized codes and L_2 normalization on the output and input to the vector quantization layer to improve performance and training stability. Additionally, the authors change the training objective, adding a logit-laplace loss and restoring the L_2 reconstruction error to $\mathcal{L}_{\text{VQGAN}}$.

Experimental Settings. We follow the open source implementation of <https://github.com/thuanz123/enhancing-transformers> and use the default model and hyperparameter settings for the small ViT-VQGAN. A complete description of the training settings can be found in Table 8 of the Appendix.

Results. Table 4 summarizes our findings. Similar to our previous results for VQ-VAEs in Section 5.1 and VQGANs in Section 5.2, codebook utilization and reconstruction metrics are significantly improved; however in this case, the quantization error is roughly the same.

5.4 VIDEO EVALUATION

Expanding our analysis beyond the image modality, we evaluate the effect of the rotation trick on video reconstructions from the BAIR Robot dataset (Ebert et al., 2017) and from the UCF101 action recognition dataset (Soomro, 2012). We follow the quantization paradigm used by ViT-VQGAN, but replace the ViT with a TimeSformer (Bertasius et al., 2021) video model. Due to compute limitations, both encoder and decoder follow a relatively small TimeSformer model: 8 layers, 256 hidden dimensions, 4 attention heads, and 768 MLP hidden dimensions. A complete description of the architecture, training settings, and hyperparameters are provided in Appendix A.5.4.

Results. Table 5 shows our results. For both datasets, training a TimeSformer-VQGAN model with the STE results in codebook collapse. We explored several different hyperparameter settings; however in all cases, codebook utilization drops to almost 0% within the first several epochs. On the other hand, models trained with the rotation trick do not exhibit any training instability and produce high quality reconstructions as indicated by r-FVD (Unterthiner et al., 2018). Several non-cherry picked video reconstructions are displayed in Appendix A.5.4.

6 CONCLUSION

In this work, we explore different ways to propagate gradients through the vector quantization layer of VQ-VAEs and find that preserving the angle—rather than the direction—between the codebook vector and gradient induces desirable effects for how points within the same codebook region are updated. Specifically, the gradient to the encoder changes as it propagates through the vector quantization

layer to push points with high distortion to new codebook regions or to pull them closer to the chosen codebook vector. The former capability corresponds to increased codebook usage and higher information capacity and the latter to decreased quantization error and lower distortion.

These effects cause a substantial improvement in model performance. Across 11 different settings, we find that training VQ-VAEs with the rotation trick improves their reconstructions. For example, training one of the VQGANs used in latent diffusion with the rotation trick improves r-FID from 5.0 to 1.6 and r-IS from 141.5 to 190.3, reduces quantization error by two orders of magnitude, and increases codebook usage by 4.5x.

REFERENCES

- Alexei Baevski, Steffen Schneider, and Michael Auli. vq-wav2vec: Self-supervised learning of discrete speech representations. *arXiv preprint arXiv:1910.05453*, 2019.
- Yoshua Bengio, Nicholas Léonard, and Aaron Courville. Estimating or propagating gradients through stochastic neurons for conditional computation. *arXiv preprint arXiv:1308.3432*, 2013.
- Gedas Bertasius, Heng Wang, and Lorenzo Torresani. Is space-time attention all you need for video understanding? In *ICML*, volume 2, pp. 4, 2021.
- Tim Brooks, Bill Peebles, Connor Holmes, Will DePue, Yufei Guo, Li Jing, David Schnurr, Joe Taylor, Troy Luhman, Eric Luhman, Clarence Ng, Ricky Wang, and Aditya Ramesh. Video generation models as world simulators. 2024. URL <https://openai.com/research/video-generation-models-as-world-simulators>.
- Huiwen Chang, Han Zhang, Lu Jiang, Ce Liu, and William T Freeman. Maskgit: Masked generative image transformer. In *Proceedings of the IEEE/CVF Conference on Computer Vision and Pattern Recognition*, pp. 11315–11325, 2022.
- Hang Chen, Sankepally Sainath Reddy, Ziwei Chen, and Dianbo Liu. Balance of number of embedding and their dimensions in vector quantization. *arXiv preprint arXiv:2407.04939*, 2024.
- Chung-Cheng Chiu, James Qin, Yu Zhang, Jiahui Yu, and Yonghui Wu. Self-supervised learning with random-projection quantizer for speech recognition. In *International Conference on Machine Learning*, pp. 3915–3924. PMLR, 2022.
- Thomas M Cover. *Elements of information theory*. John Wiley & Sons, 1999.
- Mathieu Dagréou, Pierre Ablin, Samuel Vaiter, and Thomas Moreau. How to compute hessian-vector products? In *ICLR Blogposts 2024*, 2024. URL <https://iclr-blogposts.github.io/2024/blog/bench-hvp/>. <https://iclr-blogposts.github.io/2024/blog/bench-hvp/>.
- Jia Deng, Wei Dong, Richard Socher, Li-Jia Li, Kai Li, and Li Fei-Fei. Imagenet: A large-scale hierarchical image database. In *2009 IEEE conference on computer vision and pattern recognition*, pp. 248–255. Ieee, 2009.
- Prafulla Dhariwal, Heewoo Jun, Christine Payne, Jong Wook Kim, Alec Radford, and Ilya Sutskever. Jukebox: A generative model for music. *arXiv preprint arXiv:2005.00341*, 2020.
- Xiaoyi Dong, Jianmin Bao, Ting Zhang, Dongdong Chen, Weiming Zhang, Lu Yuan, Dong Chen, Fang Wen, Nenghai Yu, and Baining Guo. Peco: Perceptual codebook for bert pre-training of vision transformers. In *Proceedings of the AAAI Conference on Artificial Intelligence*, volume 37, pp. 552–560, 2023.
- Alexey Dosovitskiy. An image is worth 16x16 words: Transformers for image recognition at scale. *arXiv preprint arXiv:2010.11929*, 2020.
- Frederik Ebert, Chelsea Finn, Alex X Lee, and Sergey Levine. Self-supervised visual planning with temporal skip connections. *CoRL*, 12(16):23, 2017.
- Patrick Esser, Robin Rombach, and Bjorn Ommer. Taming transformers for high-resolution image synthesis. In *Proceedings of the IEEE/CVF conference on computer vision and pattern recognition*, pp. 12873–12883, 2021.

- Tanmay Gautam, Reid Pryzant, Ziyi Yang, Chenguang Zhu, and Somayeh Sojoudi. Soft convex quantization: Revisiting vector quantization with convex optimization. *arXiv preprint arXiv:2310.03004*, 2023.
- Nabarnu Goswami, Yusuke Mukuta, and Tatsuya Harada. Hypervq: Mlr-based vector quantization in hyperbolic space. *arXiv preprint arXiv:2403.13015*, 2024.
- Robert Gray. Vector quantization. *IEEE Assp Magazine*, 1(2):4–29, 1984.
- Martin Heusel, Hubert Ramsauer, Thomas Unterthiner, Bernhard Nessler, and Sepp Hochreiter. Gans trained by a two time-scale update rule converge to a local nash equilibrium. *Advances in neural information processing systems*, 30, 2017.
- Geoffrey E Hinton and Richard Zemel. Autoencoders, minimum description length and helmholtz free energy. *Advances in neural information processing systems*, 6, 1993.
- Mengqi Huang, Zhendong Mao, Zhuowei Chen, and Yongdong Zhang. Towards accurate image coding: Improved autoregressive image generation with dynamic vector quantization. In *Proceedings of the IEEE/CVF Conference on Computer Vision and Pattern Recognition*, pp. 22596–22605, 2023.
- Minyoung Huh, Brian Cheung, Pulkit Agrawal, and Phillip Isola. Straightening out the straight-through estimator: Overcoming optimization challenges in vector quantized networks. In *International Conference on Machine Learning*, pp. 14096–14113. PMLR, 2023.
- Phillip Isola, Jun-Yan Zhu, Tinghui Zhou, and Alexei A Efros. Image-to-image translation with conditional adversarial networks. In *Proceedings of the IEEE conference on computer vision and pattern recognition*, pp. 1125–1134, 2017.
- Eric Jang, Shixiang Gu, and Ben Poole. Categorical reparameterization with gumbel-softmax. *arXiv preprint arXiv:1611.01144*, 2016.
- Justin Johnson, Alexandre Alahi, and Li Fei-Fei. Perceptual losses for real-time style transfer and super-resolution. In *Computer Vision–ECCV 2016: 14th European Conference, Amsterdam, The Netherlands, October 11–14, 2016, Proceedings, Part II 14*, pp. 694–711. Springer, 2016.
- Tero Karras. Progressive growing of gans for improved quality, stability, and variation. *arXiv preprint arXiv:1710.10196*, 2017.
- Tero Karras, Samuli Laine, and Timo Aila. A style-based generator architecture for generative adversarial networks. In *Proceedings of the IEEE/CVF conference on computer vision and pattern recognition*, pp. 4401–4410, 2019.
- Diederik P Kingma and Max Welling. Auto-encoding variational bayes. *arXiv preprint arXiv:1312.6114*, 2013.
- Alexander Kolesnikov, André Susano Pinto, Lucas Beyer, Xiaohua Zhai, Jeremiah Harmsen, and Neil Houlsby. Uvim: A unified modeling approach for vision with learned guiding codes. *Advances in Neural Information Processing Systems*, 35:26295–26308, 2022.
- Adrian Łafćucki, Jan Chorowski, Guillaume Sanchez, Ricard Marxer, Nanxin Chen, Hans JGA Dolfin, Sameer Khurana, Tanel Alumäe, and Antoine Laurent. Robust training of vector quantized bottleneck models. In *2020 International Joint Conference on Neural Networks (IJCNN)*, pp. 1–7. IEEE, 2020.
- Doyup Lee, Chiheon Kim, Saehoon Kim, Minsu Cho, and Wook-Shin Han. Autoregressive image generation using residual quantization. In *Proceedings of the IEEE/CVF Conference on Computer Vision and Pattern Recognition*, pp. 11523–11532, 2022.
- Fabian Mentzer, David Minnen, Eirikur Agustsson, and Michael Tschannen. Finite scalar quantization: Vq-vae made simple. *arXiv preprint arXiv:2309.15505*, 2023.
- Robin Rombach, Andreas Blattmann, Dominik Lorenz, Patrick Esser, and Björn Ommer. High-resolution image synthesis with latent diffusion models. In *Proceedings of the IEEE/CVF conference on computer vision and pattern recognition*, pp. 10684–10695, 2022.

- Tim Salimans, Ian Goodfellow, Wojciech Zaremba, Vicki Cheung, Alec Radford, and Xi Chen. Improved techniques for training gans. *Advances in neural information processing systems*, 29, 2016.
- K Soomro. Ucf101: A dataset of 101 human actions classes from videos in the wild. *arXiv preprint arXiv:1212.0402*, 2012.
- Yuhta Takida, Takashi Shibuya, WeiHsiang Liao, Chieh-Hsin Lai, Junki Ohmura, Toshimitsu Uesaka, Naoki Murata, Shusuke Takahashi, Toshiyuki Kumakura, and Yuki Mitsufuji. Sq-vae: Variational bayes on discrete representation with self-annealed stochastic quantization. *arXiv preprint arXiv:2205.07547*, 2022.
- Thomas Unterthiner, Sjoerd Van Steenkiste, Karol Kurach, Raphael Marinier, Marcin Michalski, and Sylvain Gelly. Towards accurate generative models of video: A new metric & challenges. *arXiv preprint arXiv:1812.01717*, 2018.
- Aaron Van Den Oord, Oriol Vinyals, et al. Neural discrete representation learning. *Advances in neural information processing systems*, 30, 2017.
- A Vaswani. Attention is all you need. *Advances in Neural Information Processing Systems*, 2017.
- Wilson Yan, Yunzhi Zhang, Pieter Abbeel, and Aravind Srinivas. Videogpt: Video generation using vq-vae and transformers. *arXiv preprint arXiv:2104.10157*, 2021.
- Jiahui Yu, Xin Li, Jing Yu Koh, Han Zhang, Ruoming Pang, James Qin, Alexander Ku, Yuanzhong Xu, Jason Baldridge, and Yonghui Wu. Vector-quantized image modeling with improved vqgan. *arXiv preprint arXiv:2110.04627*, 2021.
- Lijun Yu, José Lezama, Nitesh B Gundavarapu, Luca Versari, Kihyuk Sohn, David Minnen, Yong Cheng, Agrim Gupta, Xiuye Gu, Alexander G Hauptmann, et al. Language model beats diffusion-tokenizer is key to visual generation. *arXiv preprint arXiv:2310.05737*, 2023.
- Jiahui Zhang, Fangneng Zhan, Christian Theobalt, and Shijian Lu. Regularized vector quantization for tokenized image synthesis. In *Proceedings of the IEEE/CVF Conference on Computer Vision and Pattern Recognition*, pp. 18467–18476, 2023.
- Yue Zhao, Yuanjun Xiong, and Philipp Krähenbühl. Image and video tokenization with binary spherical quantization. *arXiv preprint arXiv:2406.07548*, 2024.
- Chuanxia Zheng and Andrea Vedaldi. Online clustered codebook. In *Proceedings of the IEEE/CVF International Conference on Computer Vision*, pp. 22798–22807, 2023.
- Zixin Zhu, Xuelu Feng, Dongdong Chen, Jianmin Bao, Le Wang, Yinpeng Chen, Lu Yuan, and Gang Hua. Designing a better asymmetric vqgan for stablediffusion. *arXiv preprint arXiv:2306.04632*, 2023.

A APPENDIX

A.1 COMPARISON WITHIN GENERATIVE MODELING APPLICATIONS

Absent from our work is an analysis on the effect of VQ-VAEs trained with the rotation trick on down-stream generative modeling applications. We see this comparison as outside the scope of this work and do not claim that improving reconstruction metrics, codebook usage, or quantization error in “Stage 1” VQ-VAE training will lead to improvements in “Stage 2” generative modeling applications.

While poor reconstruction performance will clearly lead to poor generative modeling, recent work (Yu et al., 2023) suggests that—at least for autoregressive modeling of codebook sequences with MaskGit (Chang et al., 2022)—the connection between VQ-VAE reconstruction performance and downstream generative modeling performance is non-linear. Specifically, increasing the size of the codebook past a certain amount will improve VQ-VAE reconstruction performance but make downstream likelihood-based geneative modeling of codebook vectors more difficult.

We believe this nuance may extend beyond MaskGit, and that the *desiderata* for likelihood-based generative models will likely be different than that for score-based generative models like diffusion. It is even possible that different preferences appear within the same class. For example, left-to-right autoregressive modeling of codebook elements with Transformers (Vaswani, 2017) may exhibit different preferences for Stage 1 VQ-VAE models than those of MaskGit.

These topics deserve a deep, and rich, analysis that we would find difficult to include within this work as our focus is on propagating gradients through vector quantization layers. As a result, we entrust the exploration of these questions to future work.

A.2 TREATING R AND $\frac{\|q\|}{\|e\|}$ AS CONSTANTS

In the rotation trick, we treat R and $\frac{\|q\|}{\|e\|}$ as constants and detached from the computational graph during the forward pass of the rotation trick. In this section, we explain why this is the case.

The rotation trick computes the input to the decoder \tilde{q} after performing a non-differentiable codebook lookup on e to find q . It is defined as:

$$\tilde{q} = \frac{\|q\|}{\|e\|} Re$$

As shown in Section 4, R is a function of both e and q . However, using the quantization function $\mathcal{Q}(e) = q$, we can rewrite both $\frac{\|q\|}{\|e\|}$ and R as a single function of e :

$$\begin{aligned} f(e) &= \frac{\|\mathcal{Q}(e)\|}{\|e\|} \left[I - 2 \left[\frac{e + \mathcal{Q}(e)}{\|e + \mathcal{Q}(e)\|} \right] \left[\frac{e + \mathcal{Q}(e)}{\|e + \mathcal{Q}(e)\|} \right]^T + 2\mathcal{Q}(e)e^T \right] \\ &= \frac{\|q\|}{\|e\|} R \end{aligned}$$

The rotation trick then becomes

$$\tilde{q} = f(e)e$$

and differentiating \tilde{q} with respect to e gives us:

$$\frac{\partial \tilde{q}}{\partial e} = f'(e)e + f(e)$$

However, $f'(e)$ cannot be computed as it would require differentiating through $\mathcal{Q}(e)$, which is a non-differentiable codebook lookup. We therefore drop this term and use only $f(e)$ as our approximation of the gradient through the vector quantization layer: $\frac{\partial \tilde{q}}{\partial e} = f(e)$. This approximation conveys more information about the vector quantization operation than the STE, which sets $\frac{\partial \tilde{q}}{\partial e} = I$.

A.3 PROOF THE ROTATION TRICK PRESERVES ANGLES

For encoder output e and corresponding codebook vector q , we provide a formal proof that the rotation trick preserves the angle between $\nabla_q \mathcal{L}$ and q as $\nabla_q \mathcal{L}$ moves to e . Unlike the notation in the main text, which assumes $q \in \mathbb{R}^{d \times 1}$, we use batch notation in the following proof to illustrate how the rotation trick works when training neural networks. Specifically, $q \in \mathbb{R}^{b \times d}$ and $R \in \mathbb{R}^{b \times d \times d}$ where b is the number of examples in a batch and d is the dimension of the codebook vector.

Remark 1. *The angle between q and $\nabla_q \mathcal{L}$ is preserved as $\nabla_q \mathcal{L}$ moves to e .*

Proof. With loss of generality, suppose $\|e\| = \|q\| = 1$. Then we have

$$\begin{aligned} q &= eR^T \\ \frac{\partial q}{\partial e} &= R \end{aligned}$$

The gradient at e will then equal:

$$\begin{aligned} \nabla_e \mathcal{L} &= \nabla_q \mathcal{L} \left[\frac{\partial q}{\partial e} \right] \\ &= \nabla_q \mathcal{L} [R] \end{aligned}$$

Let θ be the angle between q and $\nabla_q \mathcal{L}$ and ϕ be the angle between e and $\nabla_q \mathcal{L}$. Via the Euclidean inner product, we have:

$$\begin{aligned} \|\nabla_q \mathcal{L}\| \cos \theta &= q [\nabla_q \mathcal{L}]^T \\ &= eR^T [\nabla_q \mathcal{L}]^T \\ &= e [\nabla_q \mathcal{L} R]^T \\ &= e [\nabla_e \mathcal{L}]^T \\ &= \|\nabla_e \mathcal{L}\| \cos \phi \end{aligned}$$

so $\theta = \phi$ and the angle between q and $\nabla_q \mathcal{L}$ is preserved as $\nabla_q \mathcal{L}$ moves to e . \square

A.4 HOUSEHOLDER REFLECTION TRANSFORMATION

For any given e and q , the rotation that aligns e with q in the plane spanned by both vectors can be efficiently computed with Householder matrix reflections.

Definition 1 (Householder Reflection Matrix). *For a vector $a \in \mathbb{R}^d$, $I - 2aa^T \in \mathbb{R}^{d \times d}$ is reflection matrix across the subspace (hyperplane) orthogonal to a .*

Remark 2. *Let $a, b \in \mathbb{R}^d$ that define hyperplanes a^\perp and b^\perp respectively. Then a reflection across a^\perp followed by a reflection across b^\perp is a rotation of 2θ in the plane spanned by a, b where θ is the angle between a, b .*

Remark 3. *Let $a, b \in \mathbb{R}^d$ with $\|a\| = \|b\| = 1$. Define $c = \frac{a+b}{\|a+b\|}$ as the vector half-way between a and b so that $\angle(a, b) = \theta$ and $\angle(a, c) = \angle(b, c) = \frac{\theta}{2}$. $(I - cc^T)$ is the Householder reflection across a^\perp and $(I - bb^T)$ is the Householder reflection across b^\perp . Therefore, $(I - cc^T)(I - bb^T)$ corresponds to a rotation of $2(\frac{\theta}{2}) = \theta$ in $\text{span}(a, b)$ so that $(I - cc^T)(I - bb^T)a = b$.*

Returning to vector quantization with $q = [\frac{\|q\|}{\|e\|} R]e$, we can write R as the product of two Householder reflection matrices. Without loss of generality, assume e and q are unit norm. Setting $r = \frac{e+q}{\|e+q\|}$ and simplifying yields:

$$R = I - 2rr^T + 2qe^T$$

A.5 TRAINING SETTINGS

We detail the training settings used in our experimental analysis in Section 5. While a text description can be helpful for understanding the experimental settings, our released code should be referenced to fully reproduce the results presented in this work.

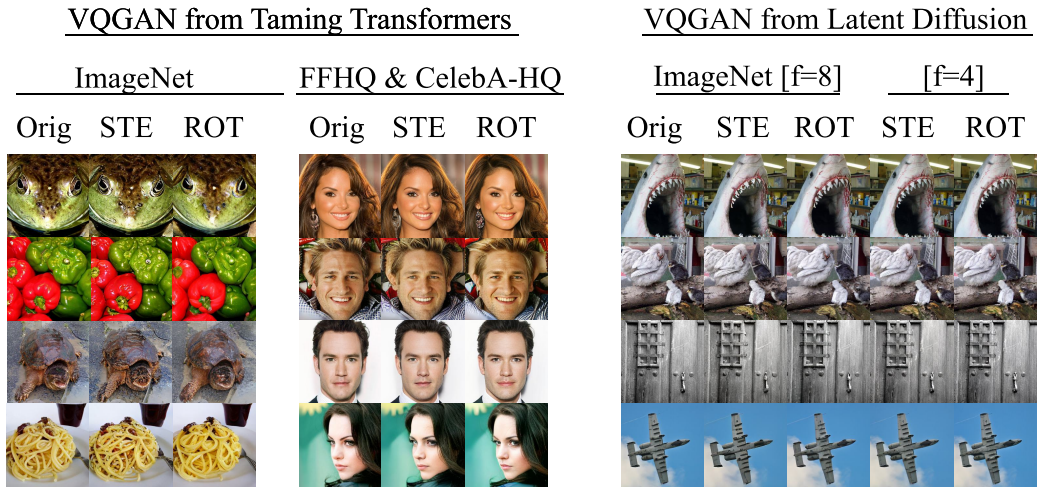


Figure 6: Non-cherry picked reconstructions for VQGAN results in Table 2 and Table 3. *ROT* is an abbreviation for the rotation trick.

A.5.1 VQ-VAE EVALUATION.

Table 6 summarizes the hyperparameters used for the experiments in Section 5.1. For the encoder and decoder architectures, we use the Convolutional Neural Network described by Esser et al. (2021). The hyperparameters for the cosine similarity codebook lookup follow from Yu et al. (2021) and the hyperparameters for the Euclidean distance codebook lookup follow from the default values set in the Vector Quantization library from <https://github.com/lucidrains/vector-quantize-pytorch>. All models replace the codebook loss with the exponential moving average described in Van Den Oord et al. (2017) with decay = 0.8. The notation for both encoder and decoder architectures is adapted from Esser et al. (2021).

Table 6: Hyperparameters for the experiments in Table 1. (1024, 32) indicates a model trained with a codebook size of 1024 and codebook dimension of 32. Similarly, (8192, 3) indicates a model trained with codebook size of 8192 and codebook dimension of 3.

	Cosine Similarity Lookup		Euclidean Lookup	
	(1024, 32)	(8192, 3)	(1024, 32)	(8192, 3)
Input size	$256 \times 256 \times 3$			
Latent size	$16 \times 16 \times 32$	$64 \times 64 \times 3$	$16 \times 16 \times 32$	$64 \times 64 \times 3$
β (commitment loss coefficient)	1.0	1.0	1.0	1.0
encoder/decoder channels	128	128	128	128
encoder/decoder channel mult.	[1, 1, 2, 2, 4]	[1, 2, 4]	[1, 1, 2, 2, 4]	[1, 2, 4]
[Effective] Batch size	256	256	256	256
Learning rate	1×10^{-4}	1×10^{-4}	5×10^{-5}	5×10^{-5}
Weight Decay	1×10^{-4}	1×10^{-4}	0	0
Codebook size	1024	8192	1024	8192
Codebook dimension	32	3	32	3
Training epochs	25	20	25	20

A.5.2 VQGAN EVALUATION

Table 7 summarizes the hyperparameters for the VQGAN experiments in Section 5.2. Non-cherry picked reconstructions for the models trained in Table 2 and Table 3 are depicted in Figure 6. As indicated by the increased r-FID score, the reconstructions out by the VQGAN trained with the rotation trick appear to better reproduce the original image, especially fine details.

Table 7: Hyperparameters for the experiments in Table 2 and Table 3. We implement the rotation trick in the open source <https://github.com/CompVis/taming-transformers> for the experiments in Table 2 and implement the rotation trick in <https://github.com/CompVis/latent-diffusion> for Table 3. In both settings, we use the default hyperparameters. \dagger : 18 epochs for ImageNet and 50 epochs for FFHQ & CelebA-HQ.

	Table 2 VQGAN	Table 3 VQGAN	Table 3 VQGAN
Input size	$256 \times 256 \times 3$	$256 \times 256 \times 3$	$256 \times 256 \times 3$
Latent size	$16 \times 16 \times 256$	$64 \times 64 \times 3$	$32 \times 32 \times 4$
Codebook weight	1.0	1.0	1.0
Discriminator weight	0.8	0.75	0.6
encoder/decoder channels	128	128	128
encoder/decoder channel mult.	[1, 1, 2, 2, 4]	[1, 2, 4]	[1, 2, 2, 4]
[Effective] Batch size	48	16	16
[Effective] Learning rate	4.5×10^{-6}	4.5×10^{-6}	4.5×10^{-6}
Codebook size	1024	8192	16384
Codebook dimensions	256	3	4
Training Epochs	18/50 \dagger	4	4

Table 8: Hyperparameters for the experiments in Table 4.

	ViT-VQGAN Settings
Input size	$256 \times 256 \times 3$
Patch size	8
Encoder / Decoder Hidden Dim	512
Encoder / Decoder MLP Dim	1024
Encoder / Decoder Hidden Depth	8
Encoder / Decoder Hidden Num Heads	8
Codebook Dimension	32
Codebook Size	8192
Codebook Loss Coefficient	1.0
Log Laplace loss Coefficient	0.0
Log Gaussian Coefficient	1.0
Perceptual loss Coefficient	0.1
Adversarial loss Coefficient	0.1
[Effective] Batch size	32
Learning rate	1×10^{-4}
Weight Decay	1×10^{-4}
Training epochs	10

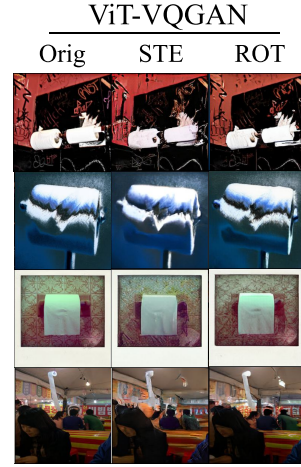


Figure 7: Non-cherry picked reconstructions for ViT-VQGAN results in Table 4. *ROT* is an abbreviation for the rotation trick.

A.5.3 ViT-VQGAN EVALUATION

Our experiments in Section 5.3 use the ViT-VQGAN implemented in the open source repository <https://github.com/thuanz123/enhancing-transformers>. The default hyperparameters follow those specified by Yu et al. (2021), and our experiments use the default architecture settings specified by the ViT small model configuration file.

We depict several reconstructions in Figure 7 and see that the ViT-VQGAN trained with the rotation trick is able to better replicate small details that the ViT-VQGAN trained with the STE misses. This is expected as the rotation trick drops r-FID from 29.2 to 11.2 as shown in Table 4.

A.5.4 TIMESFORMER VIDEO EVALUATION

We use the Hugging Face implementation of the TimeSformer from https://huggingface.co/docs/transformers/en/model_doc/timesformer and the ViT-VQGAN vector quantization layer from <https://github.com/thuanz123/enhancing-transformers>. We loosely follow the hyperparameters listed in Yu et al. (2021) and implement a small TimeSformer encoder and decoder due to GPU VRAM constraints.

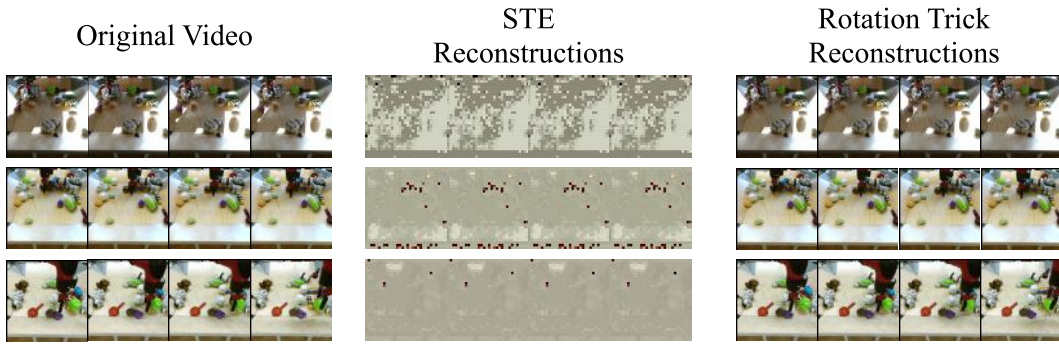


Figure 8: BAIR Robot Pushing reconstruction examples. While the model trains on 16 video frames at a time, we only visualize 4 at a time in this figure. The model trained with the STE undergoes codebook collapse, using 4 out of the 1024 codebook vectors for reconstruction and therefore crippling the information capacity of the vector quantization layer. On the other hand, the VQ-VAE trained with the rotation trick instead uses an average of 441 of the 1024 codebook vectors in each batch of 2 example videos.

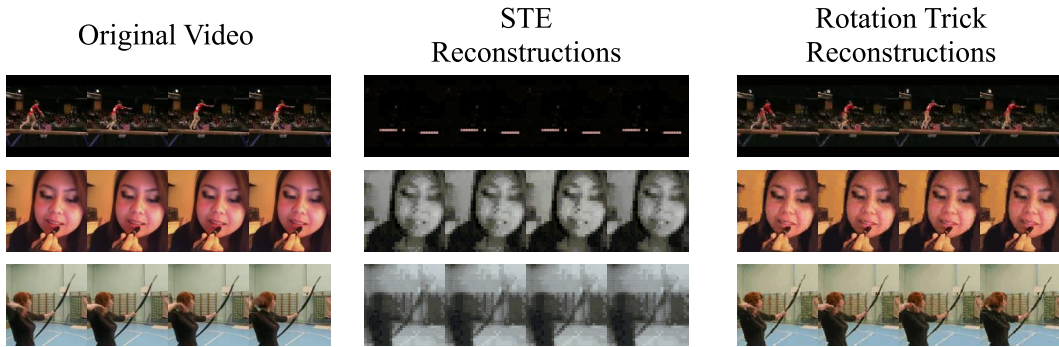


Figure 9: UCF-101 reconstruction examples. While the model trains on 16 video frames at a time, we only visualize 4 at a time in this figure. The model trained with the STE undergoes codebook collapse, using approximately 2 out of the 2048 codebook vectors for reconstruction and therefore crippling the information capacity of the vector quantization layer. The VQ-VAE trained with the rotation trick instead uses an average of 615 of the 2048 codebook vectors in each batch of 2 example videos.

We reuse the dataloading functions of both BAIR Robot Pushing and UCF101 dataloaders from [Yan et al. \(2021\)](#) at <https://github.com/wilson1yan/VideoGPT>. A complete description of the settings we use for the experiments in Section 5.4 are listed in Table 9.

We also visualize the reconstructions for the TimeSformer-VQGAN trained with the rotation trick and the STE. Figure 8 shows the reconstructions for BAIR Robot Pushing, and Figure 9 shows the reconstructions for UCF101. For both datasets, the model trained with the STE undergoes codebook collapse early into training. Specifically, it learns to only use $\frac{4}{1024}$ of the available codebook vectors for BAIR Robot Pushing and $\frac{2}{2048}$ for UCF101 in a batch of 2 input examples. Small manual tweaks to the architecture and training hyperparameters did not fix this issue.

In contrast, VQ-VAEs trained with the rotation trick do not manifest this training instability. Instead, codebook usage is relatively high—at 43% for BAIR Robot Pushing and 30% for UCF101—and the reconstructions accurately match the input, even though both encoder and decoder are very small video models.

Table 9: Hyperparameters for the experiments in Table 5. A TimeSformer (Bertasius et al., 2021) is used for the Encoder and Decoder architecture as implemented at https://huggingface.co/docs/transformers/en/model_doc/timesformer. The vector quantization layer between Encoder and Decoder follow from Yu et al. (2021) as implemented in <https://github.com/thuanz123/enhancing-transformers>.

	TimeSformer-VQGAN Settings	
	BAIR Robot Pushing	UCF101 Action Recognition
Input size	$16 \times 64 \times 64 \times 3$	$16 \times 128 \times 128 \times 3$
Patch size	2	4
Encoder / Decoder Hidden Dim	256	256
Encoder / Decoder MLP Dim	768	768
Encoder / Decoder Hidden Depth	8	8
Encoder / Decoder Hidden Num Heads	4	4
Codebook Dimension	32	32
Codebook Size	1024	2048
Codebook Loss Coefficient	1.0	1.0
Log Laplace loss Coefficient	0.0	0.0
Log Gaussian Coefficient	1.0	1.0
Perceptual loss Coefficient	0.1	0.1
Adversarial loss Coefficient	0.1	0.1
[Effective] Batch size	24	20
Learning rate	1×10^{-4}	4.5×10^{-6}
Weight Decay	1×10^{-4}	1×10^{-4}
Training epochs	30	3